Journal of Cerebral Blood Flow and Metabolism
20:736–746 © 2000 The International Society for Cerebral Blood Flow and Metabolism
Published by Lippincott Williams & Wilkins, Inc., Philadelphia

Extracellular–Intracellular Distribution of Glucose and Lactate in the Rat Brain Assessed Noninvasively by Diffusion-Weighted ^{1}H Nuclear Magnetic Resonance Spectroscopy *In Vivo*

Josef Pfeuffer, Ivan Tkáč, and Rolf Gruetter

Center for Magnetic Resonance Research, University of Minnesota Medical School, Minneapolis, Minnesota, U.S.A.

Summary: To determine the distribution of cerebral glucose and lactate between the intracellular and the extracellular space of the rat brain *in vivo*, the diffusion characteristic of glucose and lactate was compared with that of metabolites known to be mainly intracellular (*N*-acetylaspartate, choline, creatine, glutamate, *myo*-inositol, and taurine) using a pulsed-field-gradient ^{1}H nuclear magnetic resonance technique. The detection of a glucose signal at large diffusion weighting provided direct experimental evidence of *intracellular* glucose in the rat brain. At large diffusion weighting, the apparent diffusion coefficient (ADC) of glucose and lactate was similar to that of the intracellular metabolites such as *N*-acetylaspartate, creatine, and glutamate. At small diffusion weighting, the ADC of glucose and lactate was increased, which was explained by a decreased relative contribution of intracellular glucose to the total signal. The calculated extracellular volume fraction of glucose (0.19 ± 0.05) and lactate (0.17 ± 0.06) was consistent with a substantial fraction of glucose and lactate signals being intracellular. The findings were direct *in vivo* evidence that the largest concentration gradient of glucose is at the blood–brain barrier and that glucose is evenly distributed in the brain *in vivo* between the intracellular and extracellular space. **Key Words:** Intracellular glucose—Distribution space—Intracellular volume fraction—Cerebral metabolites—Rat brain *in vivo*—Diffusion-weighted ^{1}H nuclear magnetic resonance spectroscopy.

It is generally assumed that the distribution volume of glucose (Glc) in the brain is similar to that of water (Lund-Andersen, 1979; Gjedde, 1992), demonstrated by biochemical extraction studies and indirect kinetic evidence (Gjedde and Diemer, 1983; Holden et al., 1991; Gruetter et al., 1996), and that Glc phosphorylation is rate-limiting for metabolism (Furler et al., 1991). Recent noninvasive studies suggest that Glc from blood initially enters a substantial compartment fast (Knudsen et al., 1990; Hasselbalch et al., 1996) and that the brain Glc concentration is a linear function of the Glc concentration in the blood (Gruetter et al., 1998*a*). These studies are consistent with a significant fraction of Glc being in the extracellular space. Changes in extracellular Glc concentration were measured with microelectrodes or microdialysis (Silver and Erecinska, 1994; Forsyth, 1996; Lowry et al., 1998). The direct assessment of intracellular Glc was reported for cell cultures (Foley et al., 1980; Teusink et al., 1998). Because of its fast turnover, the design of studies to separate Glc from different compartments in the brain (e.g., glia–neuron or intracellular–extracellular) is difficult, and autoradiography and biochemical methods have been used, which require postmortem analysis (Gjedde, 1992). Most noninvasive *in vivo* studies assess whole-tissue properties, for example, the determination of the brain Glc concentration, by nuclear magnetic resonance (NMR) spectroscopy (Gruetter et al., 1992; Gruetter et al., 1999 and references therein).

With diffusion-weighted ^{1}H NMR spectroscopy, the intracellular signal has been previously separated from the extracellular signal because the apparent diffusion coefficient (ADC, D^{app}) in the intracellular compartment is one order of magnitude lower at large diffusion weighting (van Zijl et al., 1991). Water and cerebral metabolites experience restrictions in their self-diffusion by membranes (van Zijl et al., 1994; Pfeuffer et al.,

Received September 13, 1999; final revision received December 17, 1999; accepted December 20, 1999.

Supported by National Institutes of Health Grants CA64338 and RR08079, the W. M. Keck Foundation, and the Whitaker Foundation (R.G.).

Address correspondence and reprint requests to Josef Pfeuffer, PhD, Center for Magnetic Resonance Research, University of Minnesota Medical School, 2021 Sixth Street S.E., Minneapolis, MN 55455, U.S.A.

Abbreviations used: ADC, apparent diffusion coefficient; Cho, choline-containing compounds; Cr, creatine; Glc, glucose; Glu, glutamate; Ins, *myo*-inositol; Lac, lactate; MM, macromolecule; NAA, *N*-acetylaspartate; NAAG, *N*-acetylaspartylglutamate; NMR, nuclear magnetic resonance; PCr, phosphocreatine; *T*, temperature; Tau, taurine; TE, echo time; TM, middle interval; TR, repetition time.

1998*a*), as demonstrated by NMR measurements at large diffusion weighting and varied diffusion times in immobilized cells and the rat brain (Assaf and Cohen, 1998; Pfeuffer et al., 1998*d*). Intracellular molecules show a *restricted diffusion* characteristic limiting the mean displacement of diffusing molecules at larger diffusion times. In the extracellular space, a *hindered diffusion* characteristic has been derived, the diffusion paths around the cells being longer compared with free diffusion (Nicholson and Phillips, 1981; Rusakov and Kullmann, 1998).

Substantial improvements in sensitivity and spectral resolution of localized ^{1}H NMR spectroscopy at high magnetic fields were demonstrated recently (Gruetter et al., 1998*b*), resulting in a neurochemical profile of up to 18 metabolites that can be determined simultaneously *in vivo* (Pfeuffer et al., 1999*b*). This study determines the diffusion characteristic of multiple cerebral metabolites *in vivo*, combining large diffusion weighting and the high-resolution ^{1}H NMR methods. With these techniques, the hypothesis was tested as to whether Glc and lactate (Lac) are distributed evenly between the extracellular and intracellular space. The relative extracellular volume fraction of Glc and Lac was determined on the basis of a comparison of the diffusion characteristic with that of metabolites known to be mainly intracellular. The study provides a direct experimental evidence for the quantitative, noninvasive, and localized *in vivo* detection of *intracellular* Glc in the rat brain.

MATERIALS AND METHODS

Animal preparation

Experiments were performed according to procedures approved by the Institutional Review Board's animal care and use committee. Male Sprague-Dawley rats (230 to 300 g, n = 20) were anesthetized by a gas mixture (O_2:N_2O = 3:2) with 2% isofluorane. The rats were ventilated at physiologic conditions by a pressure-controlled respirator (Kent Scientific Corp., Litchfield, CT, U.S.A.). The oxygen saturation was maintained above 95% and was continuously monitored by a pulse oximeter with its infrared sensor attached to the tail (Nonin Medical, Inc., Minneapolis, MN, U.S.A.). The body temperature was maintained at 37°C by warm water circulation and verified by a rectal thermosensor (Cole Parmer, Vernon Hills, IL, U.S.A.). Femoral arterial and venous lines were used for regular blood gas analysis ($Pao_2 \approx$ 140 to 160 mm Hg, $Paco_2 \approx$ 35 to 40 mm Hg, pH ≈ 7.3 to 7.4) and intravenous infusion of Glc, respectively. Hyperglycemia was achieved by infusing Glc intravenously at 16 mg/min administered according to a previously described protocol (Patlak and Pettigrew, 1976).

^{1}H NMR spectroscopy

All experiments were performed on a Varian INOVA spectrometer (Varian, Palo Alto, CA, U.S.A.) interfaced to a 9.4-tesla magnet with 31-cm horizontal bore size (Magnex Scientific, Abingdon, UK). The actively shielded gradient coil (11-cm inner diameter) was capable of switching 300 mT/m field gradients in 500 microseconds (Magnex Scientific, Abingdon, UK). Eddy current effects were minimized using methods and procedures described elsewhere (Terpstra et al., 1998). For radiofrequency transmission and reception at 400 MHz, a quadrature surface coil was used consisting of two geometrically decoupled turns with 14-mm diameter, constructed according to a previously described design (Adriany and Gruetter, 1997). The localization method was based on a STEAM sequence (*ST*imulated *E*cho *A*cquisition *M*ode) using asymmetric pulses as described previously (Tkáč et al., 1999). The voxel was positioned on the midline 2 mm posterior and 3 mm ventral to the bregma. The line width of the singlet ^{1}H metabolite resonances was 8 to 12 Hz (0.02 to 0.03 ppm) *in vivo*.

Diffusion weighting

As described previously (Callaghan, 1991), unipolar gradients for diffusion weighting of the ^{1}H NMR signals of water and metabolites were placed during the τ delay in the STEAM sequence 90°–τ–90°–TM–90°–τ. The strength of the ^{1}H diffusion attenuation was characterized by the parameter b, which subsumed the diffusion time $t_D = \Delta - \delta/3$, as well as the gradient strength G, duration δ, and separation Δ, $b = (\gamma^2 \cdot G^2 \cdot \delta^2) \cdot t_D$. Units of the diffusion coefficient and the b value were $[D] = \mu m^2/ms = 10^{-9}$ m^2/s and $[b] = ms/\mu m^2 = 10^9$ s/m^2. Experiments were performed with constant diffusion time t_D, whereby the gradient strength was varied. In the first type of experiment, a b range from 0 to 5 ms/μm^2 was covered, linearly increasing G (eight points). In the second type of experiment, four b values were chosen, at $b = 0$ as a reference and at 15, 30, and 50 ms/μm^2. In both types of experiments, the signals were recorded interleaved at different b values with δ = 8 milliseconds, t_D = 119 milliseconds, TE = 22 milliseconds, and TR = 4 seconds. Gradients were applied in all three directions simultaneously.

Experimental performance of the diffusion weighting was tested and calibrated in phantoms. The signal attenuation of water and trimethylphosphate was strictly monoexponential with diffusion coefficients of (1.97 ± 0.006) and (0.437 ± 0.0006) μm^2/ms (mean ± SEM, T = 19°C). Diffusional anisotropy of the water signal in the specific voxel location *in vivo* was found to be 10% to 20% in x, y, and z direction (Pfeuffer et al., 1999*a*). Therefore, anisotropy effects of the metabolite diffusion in that voxel were considered negligible in our study.

Data analysis and quantification

Diffusion-weighted ^{1}H NMR spectroscopy is extremely sensitive to small movements in a living animal. When simply summing the acquired data, the ensuing scan-to-scan phase variations lead to a decrease in intensity in the ^{1}H metabolite spectra. This effect increased with larger diffusion weighting. To allow individual phase corrections, the data of each scan were stored separately. The sensitivity permitted the correction of the phase of single-scan metabolite spectra at all b values despite a fully suppressed water signal. The interface software for data conversion and processing was implemented with PV-WAVE (Visual Numerics, Inc., Boulder, CO, U.S.A.). Automatic phase correction of each spectrum before averaging therefore minimized signal loss from motion. Quantitatively, the additional decrease in metabolite signal intensity without the phase tracking procedure was approximately 10% at b = 5 ms/μm^2 and overestimated the apparent diffusion coefficients D^{app}, for example, of *N*-acetylaspartate (NAA) by 16%. Likewise, signal intensity was decreased by 60% at b = 50 ms/μm^2 and overestimated the D^{app} of NAA by 48% (data not shown).

Quantification of metabolite concentrations was based on frequency domain analysis using LCModel (*L*inear *C*ombination of *Model* spectra of metabolite solutions *in vitro*) (Provencher, 1993), implemented at 9.4 Tesla as described

elsewhere (Pfeuffer et al., 1999*a*). Briefly, *in vivo* spectral resonances were deconvoluted using a set of *in vitro* basis spectra by means of a constrained regularization algorithm. The method uses a linear combination of the experimentally determined spectral pattern of each metabolite. *In vitro* data were collected from NAA, *N*-acetylaspartylglutamate (NAAG), alanine, γ-aminobutyric acid, aspartate, choline-containing compounds (Cho), creatine (Cr), Glc, glutamine (Gln), glutamate (Glu), glutathione (GSH), *myo*-inositol (Ins), *scyllo*-inositol, Lac, phosphocreatine (PCr), phosphorylethanolamine (PE), and taurine (Tau). The underlying macromolecule (MM) background with a short T_1 relaxation time was determined by minimizing the metabolite signals in an inversion recovery experiment with a suitable inversion recovery delay, and included as a MM model spectrum in the LCModel basis set (Pfeuffer et al., 1999*b*). The full spectral pattern of the metabolites was analyzed with LCModel to evaluate the overall metabolite intensities, which provided a higher precision than the evaluation of intensities from single, partially overlapping peaks.

For tests of statistical significance, two-tailed Student's *t* tests and one-way analysis of variance were used (Microcal Origin, Northampton, MA, U.S.A.).

Modeling

Although the current study design is based on a model-free approach by comparing the diffusion behavior of Glc and Lac to that of known intracellular metabolites, in this section we consider the differential effect of intracellular versus extracellular diffusion on the signal attenuation. Based on previous studies (van Zijl et al., 1994; Pfeuffer et al., 1998*c*, 1998*d* and references therein), the diffusion of metabolites in brain tissue is here described by two different characteristics: restricted diffusion in the intracellular space, and hindered diffusion in the extracellular space.

Intracellular diffusion. Assuming sufficiently long diffusion times, intracellular metabolites encounter restrictions by cellular boundaries, and the mean displacement r is limited by the cell dimensions. The apparent diffusion coefficient D^{app}—determined from the slope of an experiment at a fixed diffusion time t_D—is an order of magnitude lower than that of free diffusion and defines the apparent displacement r^{app} by the Einstein equation:

$$r^{app} = \sqrt{2 \cdot D^{app} \cdot t_D} \qquad (1)$$

Although a detailed theoretical description includes a distribution of cell dimensions and spatial anisotropy as well as subcellular compartmentation and potential exchange between different compartments (Stanisz et al., 1997; Price et al., 1998; Pfeuffer et al., 1999*a*), the simplest phenomenologic model was used here. The diffusion attenuation of the signal of intracellular metabolites (components 1 and 2) with fractions p^{intra} is defined as follows:

$$S^{intra}(b) = p_1^{intra} \cdot \exp(-b \cdot D_1^{intra}) + p_2^{intra} \cdot \exp(-b \cdot D_2^{intra}) \qquad (2)$$

The fractions p_2 and $p_1 = 1 - p_2$, as well as the diffusion coefficients D_1 and D_2, were empirically determined from the diffusion behavior of known intracellular metabolites. The fraction p_i, which reflects relative signal contribution, is referred to as "apparent volume fraction" and is given as a percentage throughout the text.

Extracellular diffusion. The diffusion characteristic in the extracellular space is different because the mean displacement r^{app} is not limited with increasing diffusion time. The longer diffusion paths in the extracellular space (denoted by subscript 0) result in a hindered extracellular diffusion and a reduced diffusion coefficient compared with the free self-diffusion. The expected extracellular ADC was calculated from the self-diffusion coefficient using a tortuosity factor λ, which has been experimentally determined for healthy adult rat brain tissue to be approximately 1.5 (Nicholson and Sykova, 1998; Pfeuffer et al., 1998*a*):

$$S^{extra}(b) = p_0^{extra} \cdot \exp(-b \cdot D_0^{extra}), \quad D_0^{extra} = \frac{D_0^{free}}{\lambda^2}, \quad \lambda \geq 1 \qquad (3)$$

Diffusion of glucose and lactate. For metabolites such as Glc and Lac with both intracellular and extracellular signal contributions, the total signal is described by the superposition of extracellular and intracellular signal, that is, $S = S^{extra} + S^{intra}$ and $p_0^{extra} + p_1^{intra} + p_2^{intra} = 1$. With an estimated D_0^{extra} ranging from 0.3 to 0.5 μm²/ms ($D_0^{free} = 0.75$ to 1.1 μm²/ms), which is at most a factor of two larger than the experimentally determined D_1^{intra} (Table 2), a triexponential fit was not considered to reliably discriminate between D_0^{extra} and D_1^{intra} within the experimental error. Therefore, a biexponential fit was used:

$$S = p_1^{app} \cdot \exp(-b \cdot D_1^{app}) + p_2^{app} \cdot \exp(-b \cdot D_2^{app}), \quad p_1^{app} + p_2^{app} = 1 \qquad (4)$$

The apparent diffusion coefficient D_1^{app}, approximately a weighted average of D_0^{extra} and D_1^{intra}, and the apparent volume fraction $p_1^{app} = p_0^{extra} + p_1^{intra}$ then subsumed the extracellular contributions.

To extract the extracellular volume fraction p_0^{extra} from the data, the following calculation was used. For *intracellular* metabolites such as NAA, p_0^{extra} was assumed to be negligible, and $p_1^{app} = p_1^{intra}$ and $p_2^{app} = p_2^{intra}$. We defined a "intracellular component ratio" κ^{intra}, averaged over all intracellular metabolite data,

$$\kappa^{intra} = p_1^{intra}/p_2^{intra} \qquad (5)$$

which is a phenomenologic constant characterizing the diffusion characteristic of the two intracellular components at the given experimental conditions (i.e., diffusion time and b range). When a similar restricted diffusion characteristic in the intracellular compartments for the considered metabolites is assumed, the relative extracellular fraction is given by

$$p_0^{extra} = 1 - p_2^{app} \cdot (\kappa^{intra} + 1) \qquad (6)$$

where k^{intra} was determined from the data of intracellular metabolites, (Eq. 2 and 5), that is, $p_0^{extra} = 0$. The parameter p_2^{app} was fitted by nonlinear least square analysis of the experimental data to the biexponential decay function defined in Eq. 4.

In summary, the extracellular volume fraction p_0^{extra} of metabolites with extracellular contributions was calculated from the relative volume fraction p_2^{app} at large diffusion weighting.

Fitting

Log-linear fit. The apparent diffusion coefficients (ADC, D^{app}) of the metabolites were determined from the negative slope of the signal attenuation versus b value, that is, $\ln S = -b \cdot D^{app}$.

Log-linear regression was used for both of the experiments, that is, for data in the b range of 0 to 5 and 15 to 50 ms/μm². By convention, the apparent diffusion coefficient was termed ADC at small b values as used in previous studies. In our

biexponential model, we used D_i^{app} with the index indicating the corresponding component. To justify a log-linear fit as an approximation for the second component of a biexponential decay, it was assumed that the contributions of the first component (Eq. 4) were less than 5% for $b > 15$ ms/μm^2 corresponding to a lower limit for D_1^{app} of 0.2 μm^2/ms.

Biexponential fit. The pooled data in the full b range of 0 to 50 ms/μm^2 were analyzed by biexponential fitting constraining the sum of the volume fractions to 1 ($p_1 + p_2 = 1$). To establish statistical significance for the model parameters p_2^{app}, D_1^{app}, and D_2^{app} of the biexponential fit, a Monte Carlo simulation was performed with 10^4 trials, as described previously (Press et al., 1992). The scatter of the signal intensities at each b value was approximated with a Gaussian distribution having a SD, which was calculated from the experimental data. The confidence region ellipses were calculated in the two-dimensional parameter space (p_2^{app}, D_2^{app}) for each metabolite by a two-dimensional probability distribution and two-dimensional Gaussian fit. This method allowed determination of the probability that groups of metabolites in the (p_2^{app}, D_2^{app}) parameter space are different, despite a covariance between the model parameters.

RESULTS

The cerebral metabolite concentrations in the volume-of-interest, as determined by LCModel analysis (Pfeuffer et al., 1999*b*), were consistent with biochemical literature data. The Glc concentration was (3.5 ± 0.5) mmol/g w.w. (mean ± SD, n = 10) in rats without Glc infusions, and was (8.1 ± 1.2) μmol/g wet weight (n = 17) in hyperglycemic rats with intravenous Glc infusion. The Lac concentration was (1.9 ± 0.3) μmol/g w.w. (n = 20). At TE of 20 ms, contributions of relatively broad MM resonances were recognized throughout the whole ^{1}H NMR spectrum *in vivo* from 0.8 to 4.4 ppm (Fig. 1A). Since the diffusion of MM is much slower than for metabolites, a MM model spectrum was included in the basis set of the LCModel analysis to account for these resonances, especially at large diffusion weighting.

The contribution of Glc to the *in vivo* spectrum is shown in Fig 1B. The Glc resonances were detected at 5.23 ppm (H1-α) and also at 3.95 to 3.65, 3.55 to 3.35, and 3.25 ppm. Peaks at 3.87, 3.83, 3.49, and 3.46 ppm were discernible, as indicated by the dotted lines in Fig. 1B. The Lac resonances were detected at 1.32 and 4.11 ppm (Fig. 1A). The ^{1}H NMR metabolite resonances in the rat brain *in vivo* were indicated in detail in Fig. 2A in the spectral region of 4.2 to 1.8 ppm (i.e., NAA, Cho, Cr, Gln, Glu, Ins, PCr, PE, and Tau; see legend to Fig. 2).

Diffusion characteristic of cerebral metabolites

With a diffusion weighting of $b = 5.5$ ms/μm^2 (Fig. 2B), the metabolite intensities were reduced by 40% to 50% compared with the spectrum without diffusion weighting (Fig. 2A). The diffusion attenuation (b range from 0 to 5 ms/μm^2) of NAA (2.01 ppm) and of MM resonances demonstrated that the NAA signal was reduced up to 45% corresponding to an ADC of 0.11 μm^2/ms (Fig. 3A). In contrast, the signals from MM remained almost constant in the range of b values, consistent with their large molecular weight (Behar and Ogino, 1993). The signal decays from MM with short T_1 relaxation time were monoexponential up to $b = 50$ ms/μm^2 with a diffusion coefficient of (0.0063 ± 0.0004) μm^2/ms (r^{app} = 1.2 μm), corresponding to a signal attenuation (S/S_0) of only 27% at the maximal $b = 50$ ms/μm^2.

To compare with previous *in vivo* studies of metabolite diffusion, a separate set of diffusion-weighted experiments was performed at small b values from 0 to 5 ms/μm^2.

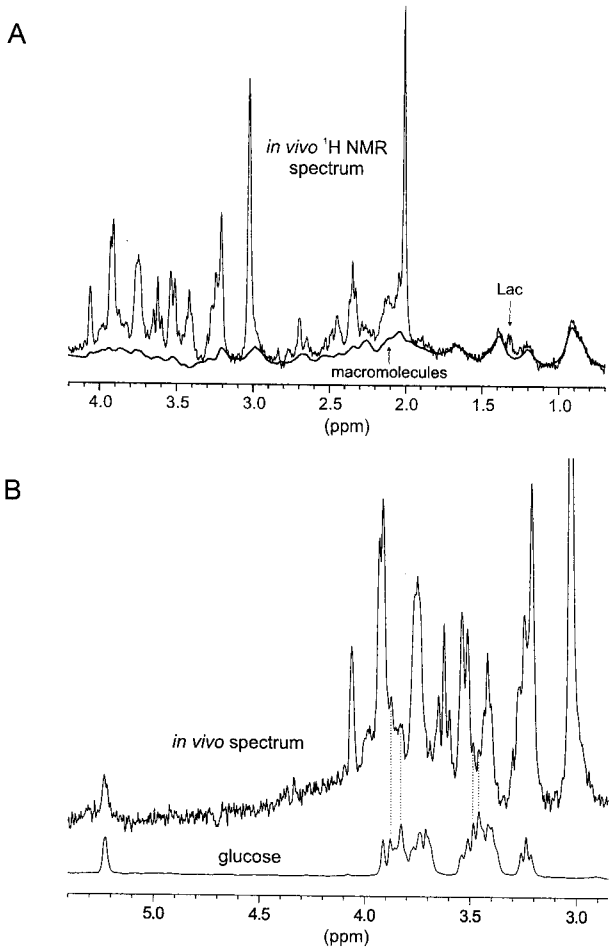

FIG. 1. Localized ^{1}H nuclear magnetic resonance (NMR) spectra of rat brain *in vivo* with the contributions of macromolecules, lactate (Lac) **(A)**, and glucose (Glc) **(B)** as analyzed with LCModel (echo time [TE] = 20 milliseconds, middle interval [TM] = 20 milliseconds, repetition time [TR] = 4 seconds). **(A)** The relatively broad resonances of the slowly diffusing macromolecules (bold curve) contribute significantly to the whole spectrum even at an TE of 20 milliseconds. **(B)** The spectral pattern of Glc was fitted through the water region at 4.65 ppm to include the Glc H1-α resonance at 5.23 ppm. Notice the resolved Glc peaks, detected at 9.4 T *in vivo* at 3.87, 3.83, 3.49, and 3.46 ppm, as indicated by the dotted lines. The Glc concentration in this spectrum was determined to be 5.2 μmol/g wet weight with Cramér-Rao lower bounds of 4%. A 1.5-Hz Gaussian line broadening and zero-order phase correction were applied.

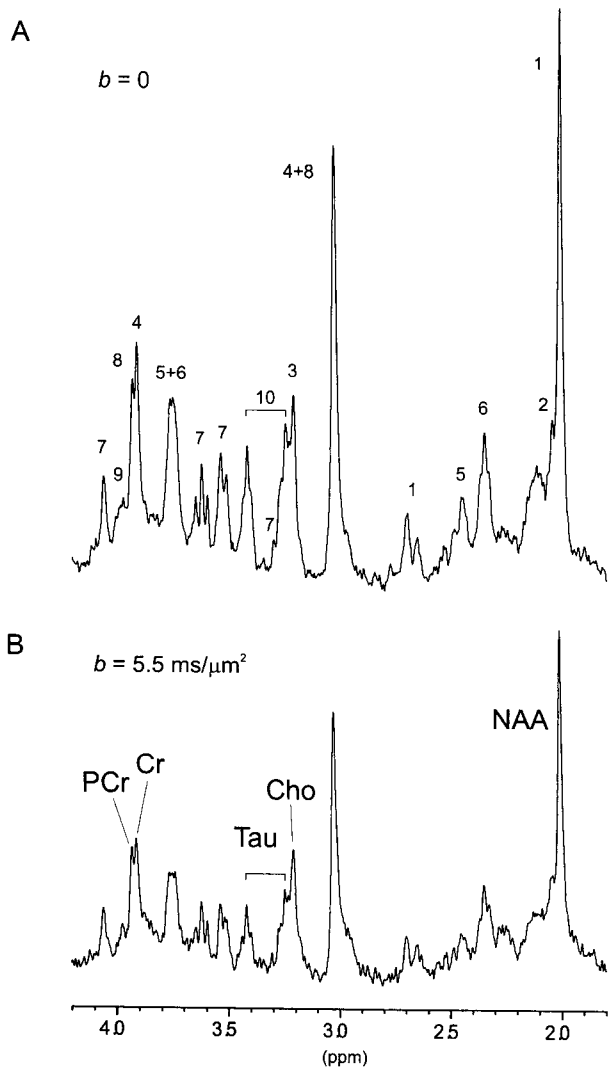

FIG. 2. The ^{1}H NMR spectra of rat brain *in vivo* without **(A)** and with **(B)** diffusion weighting b = 5.5 ms/μm^2 (t_D = 31 milliseconds, TE = 20 milliseconds, TR = 4 seconds, 128 scans). The signal attenuation of approximately 40% to 50% corresponds to an apparent diffusion coefficient of 0.09 to 0.12 μm^2/ms. Assignment of resonances (Pfeuffer et al., 1999) is indicated by the following numbers: *N*-acetylaspartate (NAA), 1; *N*-acetylaspartylglutamate (NAAG), 2; choline-containing compounds (Cho), 3; creatine (Cr), 4; glutamine (Gln), 5; glutamate (Glu), 6; *myo*-inositol (Ins), 7; phosphocreatine (PCr), 8; phosphorylethanolamine (PE), 9; and taurine (Tau), 10. Spectra were processed with 1.5-Hz Gaussian line broadening.

The signal attenuation of NAA is plotted in Fig. 4A (solid diamonds). The ADC of NAA, Glu, Cr, Ins, Tau, and GSH were between 0.10 and 0.12 μm^2/ms with errors less than 5% (Table 1). The excellent interassay reproducibility can be assessed from the fact that normalized signal intensities (e.g., of NAA, Cr + PCr, and Glu) were not distinguishable between metabolites and between different rats (data not shown).

Glucose (open squares) and Lac (cross symbols) and their fitted curves for the ADC (solid and dashed lines) are presented in Fig. 4A, with an increased signal attenuation at larger diffusion weighting compared with NAA. The relative signals of Glc and Lac at b = 2.5, 3.6, and 4.9 ms/μm^2 were lower than the NAA signals (t test, $P < 0.001$). A small 10% increase of the ADC of brain Glc with compared to without Glc infusion (Table 1) was not significant (one-way analysis of variance, $P > 0.33$).

To assess the diffusion characteristics of cerebral metabolites at large diffusion weighting, four data points with b values up to 50 ms/μm^2 were measured and normalized to S_0. The signal intensities for NAA (solid diamonds), Glc (open squares), and Lac (cross symbols) are shown in Fig. 4B (mean ± SD, n = 8) as well as the log-linear fit in the range of 15 to 50 ms/μm^2 (dotted, solid, and dashed lines). Figure 4C shows the differences

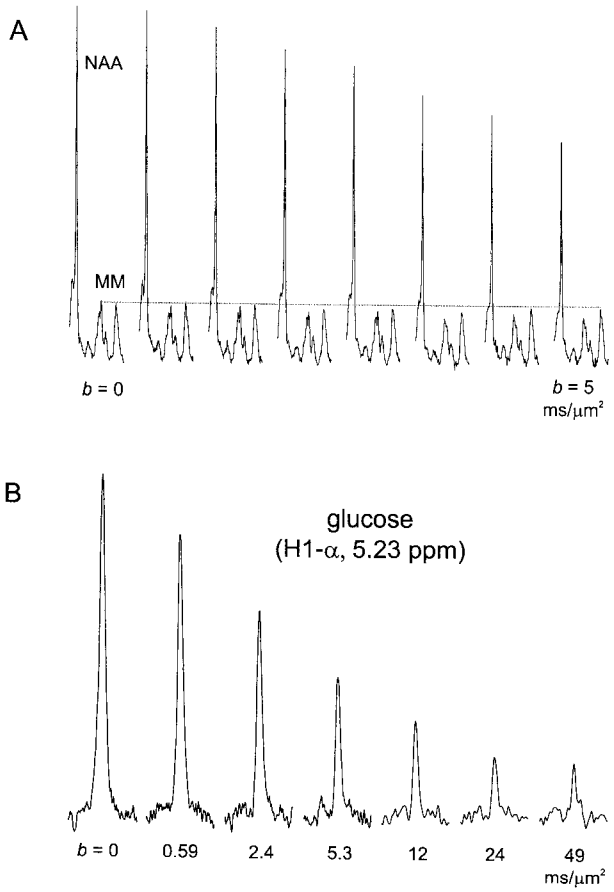

FIG. 3. Series of ^{1}H NMR spectra at increasing diffusion weighting. **(A)** In the region of 2.2 to 0.7 ppm, the dominant NAA signal is attenuated by approximately 40%, whereas the macromolecule resonances show no significant attenuation, as indicated by the dotted line (b_{max} = 5 ms/μm^2). **(B)** The diffusion attenuation of the H1-α-Glc resonance at 5.23 ppm demonstrates that resolved Glc signal can be detected at large b values up to 50 ms/μm^2. These data prove that a significant fraction of cerebral Glc *in vivo* is located in intracellular compartments being restricted in diffusion. Spectra were measured in two sets of experiments with intravenous infused Glc (first four and last three signals) and were normalized to the signal without diffusion weighting (b_{max} = 49.2 ms/μm^2, t_D = 118 milliseconds, TE = 20 milliseconds, TR = 4 seconds, 100 μL volume, 240 and 320 scans, 1.5 and 3 Hz Gaussian line broadening).

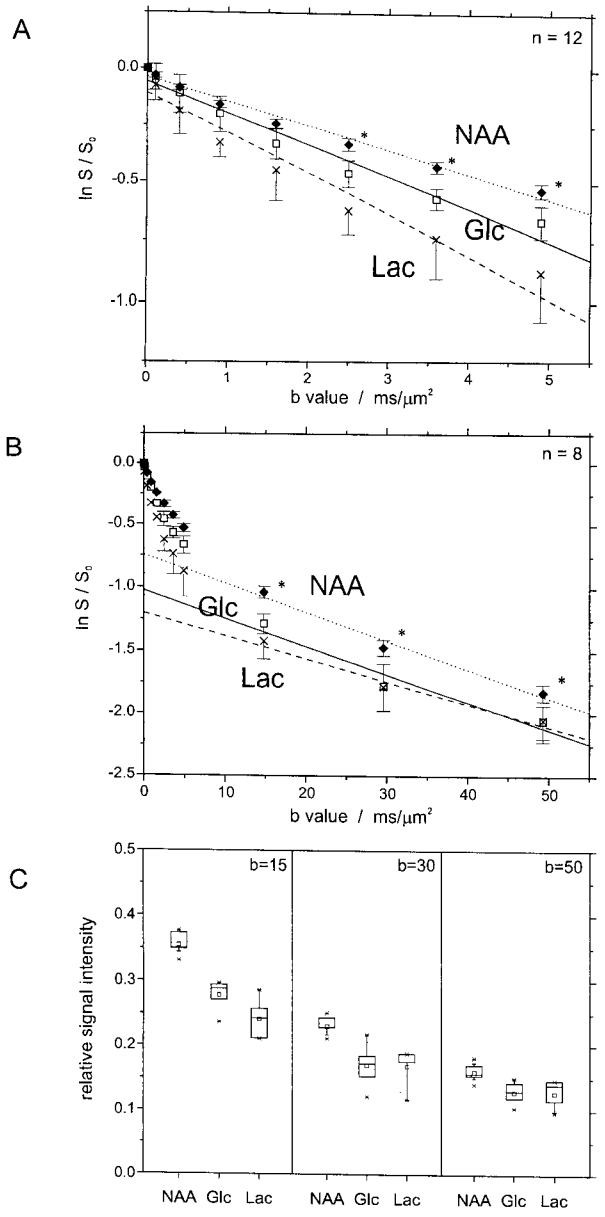

FIG. 4. Diffusion-attenuated ^{1}H NMR signal intensities of the metabolites NAA (♦), Glc (□), and Lac (×). Shown are measurements of the apparent diffusion coefficients performed at $b < 5$ ms/μm^2 **(A)**; the biexponential decay of these three metabolites when extending the b range to 50 ms/μm^2 **(B)**; and the box plots of signal intensities normalized to $S(b = 0)$ **(C)**. The apparent diffusion coefficient of Glc and Lac are larger than that of NAA and most other metabolites. Notice the equal slope at large b but different intercepts at $b = 0$, which is consistent with the different volume fraction p_2^{app} of Glc and Lac. Data were measured at seven **(A)** and three b values **(B)**, and normalized to the signal without diffusion weighting (t_D = 119 milliseconds, TE = 22 milliseconds, TR = 4 seconds). The error bars indicate the interassay variation in the log-linear plot, which are remarkably small for NAA: mean ± SD, n = 12 **(A)** and n = 8 **(B)**. For better clarity, the error bars of Lac are plotted only to the bottom, and data points from **(A)** are replotted in **(B)**. The straight lines (dotted for NAA, solid for Glc, and dashed for Lac) indicate log-linear regression. The asterisks indicate that the mean of the NAA signals is significantly different from each of the Glc and the Lac signals: t test, $P < 0.001$ **(A)**, $P < 0.002$ **(B)**. The box plots in **(C)** at b values of 15, 30, and 50 ms/μm^2 demonstrate that the normalized intensities of NAA are significantly higher than those of Glc and Lac (n = 8). The horizontal lines in the box denote the 25th, 50th, and 75th percentile values; the error bars denote the 5th and 95th percentile values. The symbol (×) denotes the 0th and 100th percentile values; the symbol (□) in the box denotes the mean of the data.

TABLE 1. *Apparent diffusion coefficient (ADC) of metabolites of ^{1}H NMR spectra in rat brain* in vivo *estimated by log-linear regression*

	Apparent diffusion coefficient (μm^2/ms)
Lac	0.176 ± 0.008
Glc*	0.139 ± 0.006
Gln	0.138 ± 0.009
PE	0.135 ± 0.007
Glc†	0.126 ± 0.010
Cr	0.120 ± 0.005
Glu	0.112 ± 0.002
NAA	0.107 ± 0.002
Ins	0.107 ± 0.003
Cr + PCr	0.106 ± 0.001
GSH	0.104 ± 0.005
Tau	0.103 ± 0.003
PCr	0.094 ± 0.003
Cho	0.093 ± 0.003
macromolecules‡	0.0063 ± 0.0004

ADCs for metabolites were fitted for each animal in the range of b = 0 to 5 ms/μm^2 and averaged (mean ± SEM, n = 12).

* ADC of glucose for rats with glucose infusion (mean ± SEM, n = 12).

† ADC of glucose for rats without glucose infusion (mean ± SEM, n = 4) being not significantly different from ADC with glucose infusion (one-way analysis of variance, $P > 0.33$).

‡ A fit range of b = 0 to 50 ms/μm^2 was used for the macromolecule intensities.

in signal intensities at the b values of 15, 30, and 50 ms/μm^2 in the box plots for NAA, Glc, and Lac, which clearly demonstrate that normalized Glc and Lac signals are significantly lower than NAA signals (t test, $P < 0.002$).

Intracellular volume fraction of cerebral glucose and lactate

Log-linear fit. The log-linear fit of the data at large b values (15 to 50 ms/μm^2) yielded D_2^{app} (slope) and p_2^{app} (intercept) for each metabolite and each animal (n = 8). The averaged p_2^{app} was (48.7 ± 0.9)% (mean ± SEM, n = 56) for the intracellular metabolites NAA, Cr, PCr, Glu, Tau, Cho, and Ins. For Glc and Lac, the D_2^{app} was similar to the grand mean of the other metabolites, but p_2^{app} was decreased (t test, $P < 0.001$) and was 37.2% ± 1.5% for Glc and 32.2% ± 2.4% for Lac (mean ± SEM, n = 8).

Biexponential fit. For a full quantitative assessment, the diffusion-weighted signals were pooled and fitted with the biexponential model of Eq. 4 (Table 2). The volume fractions p^{app} are plotted in Fig. 5A as a function of the diffusion coefficients D^{app}, indicating the fast decaying signal components (D_1^{app}) by open squares and the slow components (D_2^{app}) by solid squares. Most metabolites had volume fractions p_2^{app} around 50% (shaded areas). In an enlarged view (Fig. 5B), the slowly decaying components provided a p_2^{app} of 50.2% ± 1.1% and a D_2^{app} of 0.028 ± 0.005 mm^2/ms (all metabolites except

TABLE 2. *Apparent diffusion coefficients (D^{app}) and volume fractions (p^{app}) of metabolites of ^{1}H NMR spectra in rat brain* in vivo *determined by bi-exponential analysis*

	D_1^{app} (μm^2/ms)	D_2^{app} (μm^2/ms)	p_2^{app} (%)
Lac	0.62 ± 0.06	0.029 ± 0.002	42 ± 3
Glc	0.33 ± 0.02	0.026 ± 0.002	40 ± 2
Cr	0.35 ± 0.02	0.029 ± 0.002	51 ± 2
Glu	0.30 ± 0.02	0.026 ± 0.002	50 ± 2
Tau	0.29 ± 0.02	0.023 ± 0.002	51 ± 3
Cr + PCr	0.27 ± 0.01	0.027 ± 0.001	51 ± 2
NAA	0.27 ± 0.01	0.024 ± 0.001	49 ± 1
PCr	0.22 ± 0.02	0.024 ± 0.002	49 ± 3
Ins	0.24 ± 0.02	0.037 ± 0.003	49 ± 5
Cho	0.22 ± 0.03	0.034 ± 0.003	51 ± 5

Values were fitted from pooled data (n = 12 and n = 8) in the range b = 0 to 50 ms/μm^2, and $p_1^{app} + p_2^{app}$ was set to 1. The 68% confidence intervals of the model parameters were calculated by a Monte-Carlo stimulation with 10^4 trials.

Glc and Lac, mean ± SD). A different behavior was observed for Glc and Lac: the p_2^{app} were decreased (Table 2), being different from the intracellular metabolites ($P < 0.01$), which was determined from a Monte Carlo simulation of the errors in the biexponential model.

The intracellular component ratio $\kappa^{intra} = p_1^{intra}/p_2^{intra}$ (Eq. 5) was calculated from the intracellular metabolite data as 0.99 ± 0.02 (mean ± SEM, n = 8), which was incidentally near 1. Using this value as a phenomenologic constant, the relative extracellular volume fraction p_0^{extra} was estimated from Eq. 6 to be 19% ± 5% for Glc and 17% ± 6% for Lac.

DISCUSSION

Diffusion of intracellular metabolites

With localized ^{1}H NMR spectroscopy at high magnetic fields, it was possible to determine noninvasively the diffusion characteristic of metabolites in the rat brain *in vivo* such as Glc, resting Lac, Tau, Ins, glutamine, and Glu. The Glc concentrations under normal conditions were in agreement with previous values from the rat brain (Mason et al., 1992) and were elevated more than twofold in the brain with intravenous infusion of Glc. In this study, diffusion-weighted ^{1}H NMR spectroscopy has been used with a similar range of small b values compared with previous studies (Wick et al., 1995; van der Toorn et al., 1996; Duong et al., 1998; Dreher and Leibfritz, 1998; Dijkhuizen et al., 1999). Our ADC values, fitted in the range of 0 to 5 ms/μm^2, are in good agreement with these studies but with slightly lower values (Table 1). This can be explained by the longer diffusion time of 120 milliseconds used in our study compared with 10 to 20 milliseconds, which has been shown to reduce the ADC corresponding to the restricted diffusion of intracellular metabolites (Helmer et al., 1995; Assaf and Cohen, 1998; Pfeuffer et al., 1998*d*). In addition, a single-scan phase correction was applied, which generally leads to an inherent decrease in ADC by signal recovery (Posse et al., 1993; Ziegler et al., 1995). Comparing the monoexponential fits (straight lines) in Fig. 4A with the experimental points, a curvature was recognizable in the semilogarithmic plot, consistent with a multiexponential signal attenuation (Fig. 4A). Therefore, the ADC is expected to further increase when measured over an even smaller range of b values.

The diffusion attenuation for the MM signals (associated with a short T_1) was monoexponential up to 50 ms/μm^2 with a small diffusion coefficient (D = 0.006 μm^2/ms), which reflects the increased molecule size and the inherent decrease in mobility (Behar and Ogino, 1993). At b = 5 ms/μm^2, an attenuation of 3% was estimated for MM signals (Fig. 3A), supporting our as-

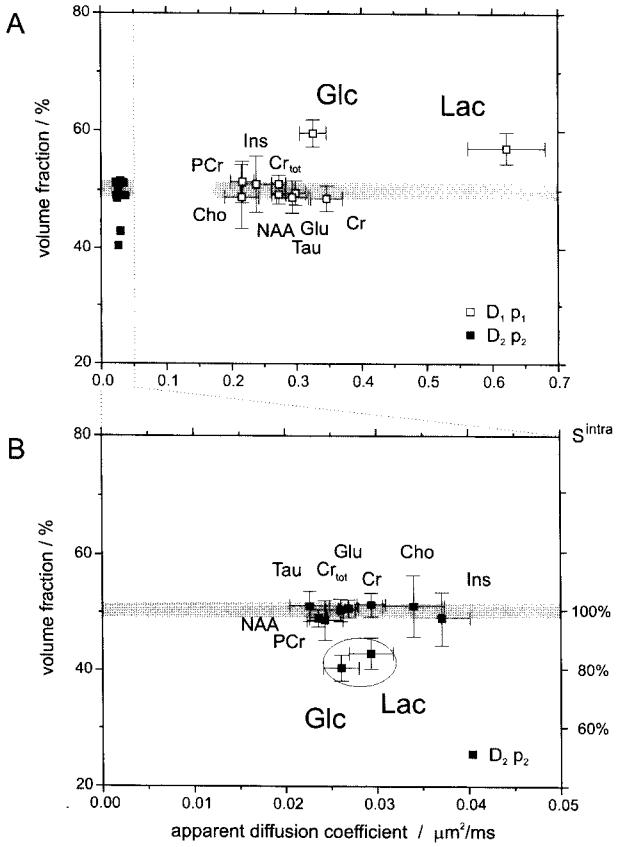

FIG. 5. Results of a biexponential analysis of the diffusion-attenuated ^{1}H NMR metabolite signal intensities in rat brain *in vivo*. **(A)** Volume fractions are plotted versus diffusion coefficients, D_1^{app} versus p_1^{app} (open symbols), and D_2^{app} versus p_2^{app} (solid symbols). The region of D_2^{app} from 0 to 0.05 mm^2/ms is expanded in **(B)**. The fractions p_2^{app} of Glc and Lac (left scale) were decreased compared with the intracellular metabolites ($P < 0.01$). The calculated relative intracellular signal $S^{intra}(b = 0)$ of Glc and Lac was approximately 80% (right scale). Probabilities have been calculated from a Monte Carlo simulation and the confidence region ellipses for each metabolite (Press et al., 1992); the error bars denote the SD of the model parameters (68% confidence interval).

sertion that signal loss from motion was minimized in our study.

Extending the diffusion weighting by a factor of 10, a biexponential attenuation was evident for all measured metabolites. Given that most metabolites (e.g., NAA or Cr) are primarily located in the intracellular space, the decrease in the apparent diffusion coefficients D^{app} must reflect the structural boundaries, characterized by the different apparent displacements r^{app} of the two components. Averaged over all intracellular metabolites, r^{app} was 8.0 ± 0.7 μm and 2.6 ± 0.2 μm for the components 1 and 2 at the diffusion time of 119 milliseconds (mean ± SD), which were calculated from the apparent diffusion coefficients D_1^{app} and D_2^{app} (Table 2) according to Eq. 1. These dimensions have been assigned to the bodies and axons of cells (Assaf and Cohen, 1998), but interpretation might be more complicated, considering a distribution of cell diameters, influences of anisotropic morphologic features (Stanisz et al., 1997), and multiple compartments (e.g., glial, neuronal, or subcellular compartments). Notice that a multiexponential signal decay in the brain may not necessarily directly reflect distinct compartments but also can be explained by the structure of restricting boundaries of a single compartment (see Pfeuffer et al., 1999*a* and references therein) such as the axons, dendrites, or glia. Analytic expressions for diffusion in two-dimensional (sheets) and one-dimensional (tubes) geometries have been calculated that are considerably non-monoexponential (Callaghan, 1991). In conclusion, caution must be used when assigning components of a multiexponential signal decay to a physiologic compartment.

Diffusion characteristic of glucose and lactate

To reduce the influence of assumptions inherent to a given model, we used the diffusion behavior of *known intracellular* metabolites as a phenomenologic standard. The similarity of p_2^{app} for all intracellular metabolites (Table 2) support our assumption that the intracellular component ratio p_1^{intra}/p_2^{intra} was constant for the overall intracellular compartment at the given experimental conditions, as evidenced by p_2^{app} being indistinguishable for most concentrated metabolites NAA, Cr, PCr, Tau, and Glu. Therefore, κ^{intra} was calculated by averaging p_1^{intra}/p_2^{intra} over all intracellular metabolites.

The observation that the ADC and D_2^{app} of most metabolites are similar (Tables 1 and 2) indicates that the diffusion barriers and cellular restrictions dominate the effect on the diffusion coefficient and that most metabolites, from a macroscopic view, can be considered to be in a similar environment (diffusion time scale of 120 milliseconds). Interestingly, Ins showed an increased D_2^{app} (but constant p_2^{app}), suggesting that it has a different intracellular distribution space. Based on measurements with cell cultures, it has been proposed recently that Ins is located mainly in the glial cells (Brand et al., 1993). In contrast, NAA, localized to the neuronal compartment (Birken and Oldendorf, 1989), has the smallest D_2^{app} compared with the other metabolites. The different D_2^{app} are consistent with a larger and smaller apparent displacement r^{app} in the glial and neuronal compartment, respectively. However, it has to be established by further experiments whether the dependency of D_2^{app} on the subcellular distribution space generally holds for all metabolites.

Both Glc and Lac exhibited a restricted diffusion characteristic similar to that of the intracellular metabolites, leading to the detection of signal at large b values and a D_2^{app} that was comparable to the intracellular metabolites (Table 2). The detection of Glc signals at large b values (Fig. 3B) is consistent with a characteristic of restricted diffusion for Glc in the intracellular space, which is described by a small D^{app} in the order of 0.02 μm^2/ms. The signals in Fig. 3B provide the direct, noninvasive evidence for a significant intracellular Glc concentration in the rat brain *in vivo* during hyperglycemia.

To assess the signal attenuation of extracellular Glc (S^{extra}, see Eq. 3), D_0^{extra} was estimated to be 0.4 μm^2/ms from the measured free diffusion constant of D_0^{free}(Glc) = 0.8 μm^2/ms (T = 37°C) using Eq. 3. A hindered diffusion characteristic was assumed for the extracellular space (λ = 1.5). At b = 5 ms/μm^2, the signal from extracellular Glc S^{extra} then was attenuated to $0.17 \cdot S_0$, and at b = 50 ms/μm^2 to $2 \cdot 10^{-8} \cdot S_0$. In the multiexponential fit, it was not possible to differentiate D_0^{extra} from D_1^{intra} because the values were close and, therefore, were fitted with a single, composite D_1^{app} (Eq. 4). For Lac, which is a smaller molecule with a larger mobility (Longsworth, 1953), the experimentally measured free diffusion constant is increased to D_0^{free}(Lac) = 1.1 μm^2/ms (T = 37°C). Therefore, the larger D_1^{app} of Lac (Table 2) is consistent with Lac being a smaller molecule than Glc.

Signal contributions from plasma Glc were considered to have a minor effect on the determination of the extracellular volume fraction of Glc. A plasma Glc concentration in vessels of about 30 mmol/L (Mason et al., 1992) averages to 0.3 to 0.6 mmol/L in brain, which was below 5% of the tissue Glc signal. In addition, the signal of plasma Glc in perfused vessels is expected to be attenuated by small diffusion gradients (Neil et al., 1994), reducing the contribution of plasma Glc to the fast decaying component well below 5%. Similarly, signal contributions of Glc from ventricles and extracerebral spaces in the midline were considered to be strongly reduced by diffusion weighting. Recent microdialysis findings (Lowry et al., 1998; McNay and Gold, 1999) show that the *extra*cellular Glc concentration in the awake rat was 0.5 to 1 mmol/L and that it is affected by neuronal activity. In our study using anesthetized animals, higher

extracellular Glc levels were measured, and similar concentrations in the extracellular and in the intracellular space were found, which was not possible to assess using microdialysis.

It has been demonstrated in several studies that the diffusion attenuation of intracellular metabolites (e.g., NAA) is multiexponential and depends on the diffusion time (Assaf and Cohen, 1998; Pfeuffer et al., 1998*d*), which is characterized by D_1^{intra} and D_2^{intra} in our model (Eq. 2). To avoid excessive dependence on theoretical models, we used the experimental diffusion attenuation curves of known intracellular metabolites as a gauge and assumed that *intra*cellular Glc or Lac has the same characteristic. This was supported by our observation that diffusion coefficients were independent of the molecule size for all concentrated intracellular metabolites. The difference between such an empirical internal standard for intracellular compounds and Glc/Lac can be explained by signal contributions from Glc and Lac in the extracellular space. Unfortunately, the estimated extracellular diffusion constant D_0^{extra} is difficult to distinguish from the intracellular diffusion component D_1^{intra}, as observed recently (Duong et al., 1998). Therefore, we assumed the extracellular diffusion to be the same as the faster decaying intracellular diffusion component. Using the slower decaying intracellular signal components (D_2^{intra}), the volume fraction p_0^{extra} of the extracellular compartment could be determined. In the study by Duong et al., a biexponential diffusion behavior was not detected with the small *b* values and short diffusion time used. The choice of the diffusion time regime is a critical parameter for the separation of hindered and restricted diffusion behavior in the brain *in vivo*, which may have masked the differences between extracellular and intracellular ADC in that study.

The anisotropy of the diffusion for water molecules was only 10% to 20% in the specific volume chosen (Pfeuffer et al., 1999*a*), which does not affect the conclusions of our report. However, no data in the literature report anisotropy for metabolites in the brain *in vivo*, such as NAA, and we are not aware of any mechanism that would cause the anisotropy being different between Glc/Lac and NAA.

The effects of transport of Glc or Lac across cell membranes were assumed to have negligible impact. An exchange of metabolites from an intracellular, highly restricted compartment to an extracellular, less restricted compartment could affect the diffusion-weighted signal attenuation, depending on the diffusion time. It has been shown that intracellular–extracellular exchange additionally attenuated the intracellular water signal at large *b* values (Pfeuffer et al., 1998*a*, 1998*e*). For metabolites, the intrinsic diffusion is about threefold slower because of the larger molecule size, and their membrane permeability is considerably decreased compared with water. Therefore, exchange effects were estimated to have a minor influence in our experiment with a diffusion-sensitive period of about 120 milliseconds.

Intracellular volume fractions

The increased ADC of Glc and Lac at small *b* values (Table 1) can be explained by a decreased fraction p_2^{app} of the component at large *b* values, whereby its slope (D_2^{app}) was not different from the intracellular metabolites (Table 2). The larger ADC of Glc and Lac also correlates with the fact that these metabolites have significant extracellular concentration in the brain. To test the hypothesis of whether diffusion properties or extracellular–intracellular volume fraction could be altered because of the hyperglycemic conditions used, the ADC of Glc at small *b* values was compared in rats without and with Glc infusion (Table 1). The unchanged ADC of Glc under both conditions strongly suggests that D_2^{app} and the extracellular–intracellular volume ratio does not change with hyperglycemia.

It has been previously pointed out that the similarity of the Glc concentration in the extracellular space compared with whole brain gave strong evidence that Glc is equally distributed in the brain and has a considerable intracellular fraction (Silver and Erecinska, 1994). The determined relative extracellular volume fraction of 19% for Glc supports this conclusion based on direct, noninvasive experimental evidence. Assuming the intracellular volume fraction in the brain to be 78% to 80% (Vorisek and Sykova, 1997), our study implies that steady-state Glc concentrations are equal in the intracellular and extracellular space within the experimental error.

Conclusions

From the observation of the Glc signals at large diffusion weighting, it can be concluded that a substantial fraction of the Glc signal is intracellular. This is further supported by the diffusion characteristic of Glc, which is similar to that of intracellular metabolites. This is the first report of a completely noninvasive simultaneous assessment of the intracellular–extracellular distribution of both Glc and Lac *in vivo*. The estimated relative extracellular signal of Glc (19%) at hyperglycemia is consistent with the relative extracellular volume and indicates that the distribution of Glc in the brain is approximately even in the extracellular and intracellular space. This supports the notion that the largest concentration gradient of Glc is at the blood–brain barrier, where the Glc concentrations are about a factor of two to three higher than in the brain (Gruetter et al., 1998*a*). These methods can be extended to assess the extracellular fraction of metabolites noninvasively and to monitor their changes in pathologic animal models, such as changes of extracellular Lac in brain lesions and tumors.

Acknowledgments: The authors thank Professors Kamil Ugurbil and Michael Garwood, Minneapolis, for support, and Professor Dieter Leibfritz, Bremen, and In-Young Choi, Minneapolis, for helpful discussions.

REFERENCES

Adriany G, Gruetter R (1997) A half-volume coil for efficient proton decoupling in humans at 4 tesla. *J Magn Reson* 125:178–184

Assaf Y, Cohen Y (1998) In vivo and in vitro bi-exponential diffusion of *N*-acetyl aspartate (NAA) in rat brain: a potential structural probe? *NMR Biomed* 11:67–74

Behar KL, Ogino T (1993) Characterization of macromolecule resonances in the ^{1}H NMR spectrum of rat brain. *Magn Reson Med* 30:38–44

Birken DL, Oldendorf WH (1989) *N*-acetyl-L-aspartic acid: a literature review of a compound prominent in ^{1}H-NMR spectroscopic studies of brain. *Neurosci Biobehav Rev* 13:23–31

Brand A, Richter-Landsberg C, Leibfritz D (1993) Multinuclear NMR studies on the energy metabolism of glial and neuronal cells. *Dev Neurosci* 15:289–298

Callaghan PT. In: *Principles of Nuclear Magnetic Resonance Microscopy.* Oxford: Clarendon Press, 1991:328–419

Dijkhuizen RM, de Graaf RA, Tulleken KA, Nicolay K (1999) Changes in the diffusion of water and intracellular metabolites after excitotoxic injury and global ischemia in neonatal rat brain. *J Cereb Blood Flow Metab* 19:341–349

Dreher W, Leibfritz D (1998) Apparent Diffusion Coefficients of Metabolites With Uncoupled and Coupled Resonances Measured in the Healthy Rat Brain by Diffusion-Weighted ^{1}H-CT-PRESS. *Proc ISMRM 6th Scientific Meeting,* Sydney, p 343

Duong TQ, Ackerman JJ, Ying HS, Neil JJ (1998) Evaluation of extra- and intracellular apparent diffusion in normal and globally ischemic rat brain via ^{19}F NMR. *Magn Reson Med* 40:1–13

Foley JE, Cushman SW, Salans LB (1980) Intracellular glucose concentration in small and large rat adipose cells. *Am J Physiol* 238:E180–E185

Forsyth RJ (1996) Astrocytes and the delivery of glucose from plasma to neurons. *Neurochem Int* 28:231–241

Furler SM, Jenkins AB, Storlien LH, Kraegen EW (1991) In vivo location of the rate-limiting step of hexose uptake in muscle and brain tissue of rats. *Am J Physiol* 261:E337–E347

Gjedde A (1992) Blood–brain glucose transfer. In: Physiology and Pharmacology of the Blood–Brain Barrier (Bradbury M, ed), New York, Springer Verlag, pp 65–117

Gjedde A, Diemer NH (1983) Autoradiographic determination of regional brain glucose content. *J Cereb Blood Flow Metab* 3:303–310

Gruetter R, Novotny EJ, Boulware SD, Rothman DL, Mason GF, Shulman GI, Shulman RG, Tamborlane WV (1992) Direct measurement of brain glucose concentrations in humans by ^{13}C NMR spectroscopy. *Proc Natl Acad Sci USA* 89:1109–1112

Gruetter R, Novotny EJ, Boulware SD, Rothman DL, Shulman RG (1996) ^{1}H NMR studies of glucose transport in the human brain. *J Cereb Blood Flow Metab* 16:427–438

Gruetter R, Ugurbil K, Seaquist ER (1998*a*) Steady-state cerebral glucose concentrations and transport in the human brain. *J Neurochem* 70:397–408

Gruetter R, Weisdorf SA, Rajanayagan V, Terpstra M, Merkle H, Truwit CL, Garwood M, Nyberg SL, Ugurbil K (1998b) Resolution improvements in in vivo ^{1}H NMR spectra with increased magnetic field strength. *J Magn Reson* 135:260–264

Gruetter R, Pfeuffer J, Tkac I, Damberg G, Seaquist ER (1999) NMR studies of *in vivo* brain glucose concentrations and transport. In: Brain Barrier Systems: Alfred Benzon Symposium 45 (Paulson O, Knudsen GM, Moos T, eds), Copenhagen, Munksgaard, pp 128–138

Hasselbalch SG, Knudsen GM, Holm S, Hageman LP, Capaldo B, Paulson OB (1996) Transport of D-glucose and 2-fluorodeoxyglucose across the blood–brain barrier in humans. *J Cereb Blood Flow Metab* 16:659–666

Helmer KG, Dardzinski BJ, Sotak CH (1995) The application of porous-media theory to the investigation of time-dependent diffusion in *in vivo* systems. *NMR Biomed* 8:297–306

Holden JE, Mori K, Dienel GA, Cruz NF, Nelson T, Sokoloff L (1991) Modeling the dependence of hexose distribution volumes in brain on plasma glucose concentration: implications for estimation of the local 2-deoxyglucose lumped constant. *J Cereb Blood Flow Metab* 11:171–182

Knudsen GM, Pettigrew KD, Paulson OB, Hertz MM, Patlak CS (1990) Kinetic analysis of blood–brain barrier transport of D-glucose in man: quantitative evaluation in the presence of tracer backflux and capillary heterogeneity. *Microvasc Res* 39:28–49

Longsworth LG (1953) Diffusion measurements, at 25°, of aqueous solutions of amino acids, peptides, and sugars. *J Am Chem Soc* 75:5705–5709

Lowry JP, O'Neill RD, Boutelle MG, Fillenz M (1998) Continuous monitoring of extracellular glucose concentrations in the striatum of freely moving rats with an implanted glucose biosensor. *J Neurochem* 70:391–396

Lund-Andersen H (1979) Transport of glucose from blood to brain. *Physiol Rev* 59:305–352

Mason GF, Behar KL, Rothman DL, Shulman RG (1992) NMR determination of intracerebral glucose concentration and transport kinetics in rat brain. *J Cereb Blood Flow Metab* 12:448–455

McNay EC, Gold PE (1999) Extracellular glucose concentrations in the rat hippocampus measured by zero-net-flux: effects of microdialysis flow rate, strain, and age. *J Neurochem* 72:785–790

Neil JJ, Bosch CS, Ackerman JJ (1994) An evaluation of the sensitivity of the intravoxel incoherent motion (IVIM) method of blood flow measurement to changes in cerebral blood flow. *Magn Reson Med* 32:60–65

Nicholson C, Phillips JM (1981) Ion diffusion modified by tortuosity and volume fraction in the extracellular microenvironment of the rat cerebellum. *J Physiol (Lond)* 321:225–257

Nicholson C, Sykova E (1998) Extracellular space structure revealed by diffusion analysis. *Trends Neurosci* 21:207–215

Patlak CS, Pettigrew KD (1976) A method to obtain infusion schedules for prescribed blood concentration time courses. *J Appl Physiol* 40:458–463

Pfeuffer J, Bröer S, Bröer A, Lechte M, Flögel U, Leibfritz D (1998*a*) Expression of aquaporins in *Xenopus laevis* oocytes and glial cells as detected by diffusion-weighted ^{1}H NMR spectroscopy and photometric swelling assay. *Biochim Biophys Acta* 1448:27–36

Pfeuffer J, Dreher W, Sykova E, Leibfritz D (1998*b*) Water signal attenuation in diffusion-weighted ^{1}H NMR experiments during cerebral ischemia: influence of intracellular restrictions, extracellular tortuosity, and exchange. *Magn Reson Imaging* 16:1023–1032

Pfeuffer J, Flögel U, Dreher W, Leibfritz D (1998*c*) Restricted diffusion and exchange of intracellular water: theoretical modelling and diffusion time dependence of ^{1}H NMR measurements on perfused glial cells. *NMR Biomed* 11:19–31

Pfeuffer J, Flögel U, Leibfritz D (1998*d*) Influences of Diffusion Time and Osmotic Stress on Intracellular Metabolite Signals in Perfused Glial Cells as Detected by Diffusion-Weighted ^{1}H NMR Spectroscopy. *Proc ISMRM 6th Scientific Meeting,* Sydney, p 533

Pfeuffer J, Flögel U, Leibfritz D (1998*e*) Monitoring of cell volume and water exchange time in perfused cells by diffusion-weighted ^{1}H NMR spectroscopy. *NMR Biomed* 11:11–18

Pfeuffer J, Provencher SW, Gruetter R (1999*a*) Water diffusion in rat brain in vivo as detected at very large b values is multicompartmental. *MAGMA* 8:98–108

Pfeuffer J, Tkac I, Provencher SW, Gruetter R (1999*b*) Toward an in vivo neurochemical profile: quantification of 18 metabolites in short-echo-time ^{1}H NMR spectra of the rat brain. *J Magn Reson* 141:104–120

Posse S, Cuenod CA, Le Bihan D (1993) Human brain: proton diffusion MR spectroscopy. *Radiology* 188:719–725

Press WH, Teukolsky SA, Vetterling WT, Flannery BP (1992) Confidence limits on estimated model parameters. In: Numerical Recipies in C: The Art of Scientific Computing, New York, Cambridge University Press, pp 689–699

Price WS, Barzykin AV, Hayamizu K, Tachiya M (1998) A model for diffusive transport through a spherical interface probed by pulsed-field gradient NMR. *Biophys J* 74:2259–2271

Provencher SW (1993) Estimation of metabolite concentrations from localized in vivo proton NMR spectra. *Magn Reson Med* 30:672–679

Rusakov DA, Kullmann DM (1998) Extrasynaptic glutamate diffusion in the hippocampus: ultrastructural constraints, uptake, and receptor activation. *J Neurosci* 18:3158–3170

Silver IA, Erecinska M (1994) Extracellular glucose concentration in mammalian brain: continuous monitoring of changes during increased neuronal activity and upon limitation in oxygen supply in normo-, hypo-, and hyperglycemic animals. *J Neurosci* 14:5068–5076

Stanisz GJ, Szafer A, Wright GA, Henkelman RM (1997) An analytical model of restricted diffusion in bovine optic nerve. *Magn Reson Med* 37:103–111

Terpstra M, Andersen PM, Gruetter R (1998) Localized eddy current compensation using quantitative field mapping. *J Magn Reson* 131:139–143

Teusink B, Diderich JA, Westerhoff HV, van Dam K, Walsh MC (1998) Intracellular glucose concentration in derepressed yeast cells consuming glucose is high enough to reduce the glucose transport rate by 50%. *J Bacteriol* 180:556–562

Tkáč I, Starcuk Z, Choi IY, Gruetter R (1999) In vivo ^{1}H NMR spectroscopy of rat brain at 1 ms echo time. *Magn Reson Med* 41:649–656

van der Toorn A, Dijkhuizen RM, Tulleken CA, Nicolay K (1996) Diffusion of metabolites in normal and ischemic rat brain measured by localized ^{1}H MRS. *Magn Reson Med* 36:914–922

van Zijl PC, Moonen CT, Faustino P, Pekar J, Kaplan O, Cohen JS (1991) Complete separation of intracellular and extracellular information in NMR spectra of perfused cells by diffusion-weighted spectroscopy. *Proc Natl Acad Sci USA* 88:3228–3232

van Zijl PC, Davis D, Moonen CT (1994) Diffusion spectroscopy in living systems. In: NMR in Physiology and Biomedicine (Gillies RJ, ed), London, Academic Press, pp 185–198

Vorisek I, Sykova E (1997) Ischemia-induced changes in the extracellular space diffusion parameters, K+, and pH in the developing rat cortex and corpus callosum. *J Cereb Blood Flow Metab* 17:191–203

Wick M, Nagatomo Y, Prielmeier F, Frahm J (1995) Alteration of intracellular metabolite diffusion in rat brain in vivo during ischemia and reperfusion. *Stroke* 26:1930–1933

Ziegler A, Izquierdo M, Remy C, Decorps M (1995) Optimization of homonuclear two-dimensional correlation methods for in vivo and ex vivo NMR. *J Magn Reson B* 107:10–18